MR-Pathological Comparison in F98-Fischer Glioma Model Using a Human Gantry

Jocelyn Blanchard, David Mathieu, Yves Patenaude, David Fortin

ABSTRACT: ***Object:*** This study reports our findings in assessing in vivo tumour growth with magnetic resonance imaging using a commercial magnet and antenna in F98 implanted Fischer rats. A comparison of T1 gadolinium-enhanced coronal MR scans and pathology specimens in corresponding animals was accomplished. ***Methods:*** One rat was used in serial experiments to establish adequate imaging parameters. Afterward, 12 animals implanted with F98 cells underwent a MR study following intervals spanning five, ten, 15 and 20 days on a 1.5T human Siemens. Using a small loop antenna, a coronal T1 weighted MRI scan with Gadolinium was performed. Images were analyzed and volumes of enhancing tumour were calculated. The animals were sacrificed after the imaging procedure and brain were harvested and processed in pathology. Pathology specimens and MR images were analyzed using image processing software. One hematoxylin + eosin (H&E) slide per specimen was compared to the corresponding MR slice depicting the largest area of enhancement. ***Results:*** The MR enhancement areas obtained were 2.18mm^2, 8.25mm^2, 21.6mm^2 and 23.17mm^2 at five, ten, 15 and 20 days. Tumour margin measurements on pathologic samples produced areas of 0.29mm^2, 4.43 mm^2, 8.3mm^2, and 12.9mm^2 at five, ten, 15 and 20 days respectively. ***Conclusion:*** The T1-enhancing images constantly overestimated the tumour bulk on H&E. This phenomenon is explained by enhancement of the brain around tumour, the extra-axial tumour growth, and a shrinking factor of 17% related to the fixation process. Nonetheless, the radiological tumour growth paralleled the histological samples. This technology is thus suitable to follow tumour growth in F98 implanted rats.

RÉSUMÉ: Comparaison de l'IRM utilisant un portique humain et de l'anatomopathologie chez un modèle animal, le gliome F98 chez le rat Fisher. ***Objet:*** Cette étude rapporte nos observations sur l'évaluation de la croissance tumorale in vivo à l'imagerie par résonance magnétique (IRM) en utilisant un aimant et une antenne commerciales chez des rats Fisher chez qui on a implanté un gliome F98. Nous avons comparé l'image coronale en pondération T1 avec injection de gadolinium et le spécimen anatomopathologique de chaque animal. ***Méthodes:*** Des essais en série sur un rat ont servi à établir les paramètres d'imagerie appropriés. Par la suite, 12 animaux chez qui on avait implanté des cellules F98 ont subi une IRM avec un appareil Siemens 1,5T utilisé chez l'humain, à intervalles de 5, 10, 15 et 20 jours. Une petite antenne en boucle a été utilisée pour obtenir l'IRM coronale avec gadolinium pondérée en T1. Les images ont été analysées et le volume de tumeur rehaussante a été calculé. Les animaux étaient sacrifiés après l'imagerie et le cerveau était prélevé et préparé en pathologie. Les spécimens anatomopathologiques et les images étaient analysées au moyen d'un logiciel de traitement d'image. Une coupe colorée en H&E de chaque spécimen a été comparée à la coupe IRM correspondante décrivant la zone de rehaussement la plus étendue. ***Résultats:*** Les zones de rehaussement à l'IRM étaient de 2,18 mm2, 8,25 mm2, 21,6 mm2 et 23,17 mm2 après 5, 10, 15 et 20 jours. La mesure du périmètre de la tumeur sur les coupes anatomopathologiques a permis d'évaluer la surface qui était de 0,29 mm2, 4,43 mm2, 8,3 mm2 et 12,9 mm2 après 5, 10, 15 et 20 jours respectivement. ***Conclusion:*** Les images rehaussées en T1 surestimaient toujours la masse tumorale mesurée sur les coupes H&E. Ce phénomène s'explique par le rehaussement du tissu cérébral autour de la tumeur, la croissance tumorale extra-axiale et un facteur de contraction de 17% dû au processus de fixation. Néanmoins, la croissance tumorale observée à l'imagerie évoluait parallèlement à celle observée en anatomopathologie. Cette technologie convient donc au suivi de la croissance tumorale chez les rats porteurs d'un implant F98.

Can. J. Neurol. Sci. 2006; 33: 86-91

The treatment of malignant glial tumours remains a tremendous challenge despite decades of pre-clinical and clinical research. These tumours represent about 80% of all primary brain tumours, and have a universally unfavourable prognosis despite new radiotherapy protocols and chemotherapy regimens.[1,2] Thus, research remains active in this field, and therefore commands for pre-clinical models that are valid and predictive. Many animal models, mostly using the rat, have been developed to simulate the behaviour of glioblastoma tumour cells and to study the impact of radiotherapy,[3] chemotherapy,[4,5] immunotherapy[6] and gene therapy.[7] The outcome surrogates most studied in these models have relied on survival time[4,8] or tumour size at histology.[9] However, depending on the size of the inoculums, the implantation technique and the model chosen, there can be a great variability in the behaviour of the tumour. The percentage of tumour take reported in various studies is

From the Divisions of Neurosurgery and Neuro-oncology, Department of Surgery (JB, DM, DF), Department of Radiology (YP), Centre Hospitalier Universitaire de Sherbrooke, Sherbrooke University, Sherbrooke, QC, Canada.

Received May 11, 2005. Accepted in final form September 24, 2005.

Reprint requests to: David Fortin, Centre Hospitalier Universitaire de Sherbrooke, 3001 12e avenue Nord, Sherbrooke, Quebec, J1H 5N4, Canada.

highly variable, ranging from 50% to 100%.[4,10,11] A considerable variation in tumour volumes can also be observed within a group of implanted animals using the same technique. A recently published study reported tumour volumes ranging from less than 10 mm^3 to more than 80 mm^3 after a standardized implantation technique and a constant observation period.[12] This thus illustrates the difficulty in interpreting response to an experimental treatment based only on the tumour size at pathology after euthanasia of the animal.

In order to minimize the impact of these variations and decrease several sources of bias that could produce false positive results, in vivo tumour assessment is mandatory in the use of these models. Magnetic resonance has become the standard imaging technology in the follow-up of brain tumours in the clinical situation. In an effort to emulate the clinical context and to validate and monitor glioma implantation models, it is thus only natural to extend the use of this imaging modality to the laboratory. Using small and powerful magnets up to 7 Tesla and custom made antennas, high resolution imaging was obtained from different groups.[13-16] This MR technology has been used to assess brain tumour formation[11] and volumes,[13,14] tumour vascularisation,[15] blood-brain barrier permeability[17,18] and responses to various therapeutic agents.[14,19] This equipment leads to very good quality imaging but is not widespread in use and is not easily available. When reviewing current literature on the subject, a trend seems to emerge in that the high field magnet technology gradually becomes a standard in animal imaging.[11,14] While this technology is doubtlessly useful, most notably for all the physiological data acquisitions, we believe that it is not mandatory for tumour follow-up assessments focusing on the size of tumour and response to treatment. Although we do not have access to high field magnet technology, we are nonetheless active in the field of neuro-oncology research.

The objectives of this study were threefold: 1) to define optimal parameters allowing imaging of the F98 Fisher glioma model with a commercially available antenna, using the 1.5T Siemens magnet MR scan available at our university center 2) to assess the accuracy of this approach in following in vivo tumour progression in the F98-Fischer model and 3) to ensure that the imaging findings match the corresponding pathology samples.

Methods

Animal model

The experimental protocol was approved by the institutional ethical committee and conformed to regulations of the Canadian Council on animal care. Thirteen adult male Fischer rats were obtained and kept in controlled conditions in our facilities.

The F98 cell line (ATCC), was grown in monolayer using a solution of Dulbecco's modified Eagle medium (DMEM) supplemented with 10% fetal bovine serum and a mix of penicillin-streptomycin. Cells were incubated at 37°C in a humidified environment with 5% CO_2 and propagated upon confluence, every three days. The implantation solution was prepared by trypsinization of the cell culture followed by resuspension in a DMEM solution free of fetal bovine serum. The solution was diluted to obtain a concentration of $1x10^4$ cells in a volume of five microliters. A trypan blue exclusion test was performed to assess cell viability before implantation.

The implantation procedures were performed under general anesthesia using an intraperitoneal injection of ketamine (87mg/kg) and xylazine (13mg/kg). A midline incision on the scalp was accomplished to expose the bregma. The rat was positioned in the stereotactic frame. Using a 16 Ga needle, a burr hole was drilled 3 mm lateral and 1 mm anterior to the bregma. A 25 Ga needle was inserted via the craniotomy at a depth of 6 mm from the external table, targeting the right caudate nucleus region. A 5 µl solution containing 10^4 cells suspended in DMEM was infused at a constant rate over five minutes using a MicroSyringe infusion pump (World Precision Instruments Inc.). After a delay of one minute, the needle was slowly withdrawn and the burr hole sealed with bone wax. The scalp was closed using a running suture. The animals were allowed to awake and were observed for a variable period.

Experimental groups

One animal was used for a series of test images to define the optimal imaging parameters. After acquiring this data, each of the 12 remaining animals was randomly assigned to one of the four experimental groups corresponding to the interval between the implantation procedure and the MRI. To permit corresponding pathological study, the animals were sacrificed immediately after the MRI. The groups were divided as follows: five, ten, 15 and 20 days.

Imaging

The test animal was anesthetized with ketamine/xylazine (as previously described for the implantation procedure) and taken to the MR suite. After a series of preliminary images, the Siemens small loop flex coil (4 cm diameter) was chosen as the ideal antenna. It was simply laid on the head of the rat and secured with tape (Figure 1). The animal was positioned inside the magnet in prone position. Images were acquired in the coronal plane. The TR and TE were varied in a series of serial test imaging until images were considered optimal, both for the

Figure 1: *Illustration of the setup used for imaging. An anesthetised Fischer rat rests prone inside the magnet with the small loop antenna simply laid on its head.*

https://doi.org/10.1017/S0317167100004753 Published online by Cambridge University Press

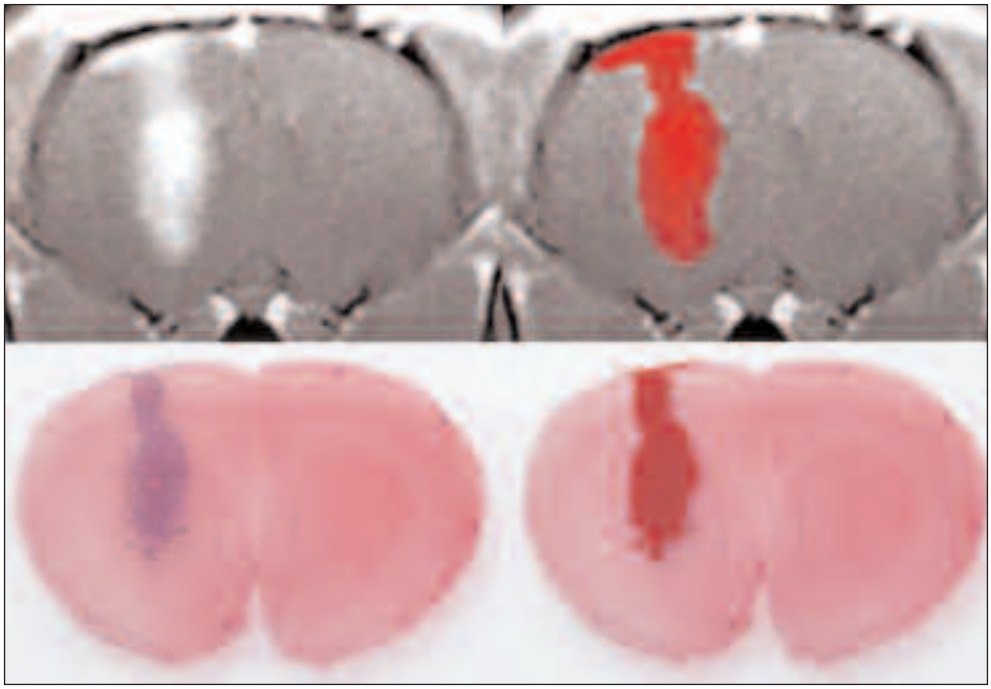

Figure 2: *Depiction of the method used to calculate tumour surface, on a coronal T1 MR scan and on the corresponding pathology sample, in an animal implanted 15 days earlier. After manually delimiting tumour contour, the software generates area measurements in pixels, later converted in mm^2.*

T1 and the T2 sequences. This implies that, once a certain point had been reached, further manipulations did not improve image quality or definition, but increased acquisition time. For T1 weighted images, the final parameters used were a TR of 400, and a TE of 17 whereas for T2 weighted images, a TR of 3340, and a TE of 99 were selected. The matrix specified was 512 x 384. Slice thickness was 2 mm and six slices per specimen were obtained. We also performed enhanced T1 weighted images with IV Gadopentetate dimeglumine. The contrast agent was injected via the penile vein (0.1 cc of a 469 mg/cc solution). The acquisition time was seven minutes for T2 and five minutes for T1 images. Using these parameters, images deemed adequate were produced in T2, T1 and T1 with gadolinium.

Pathology

After the MRI procedure, while still under general anesthesia, rats were euthanized by means of intracardiac formaldehyde perfusion. The brains were harvested and preserved in formalin solution. The specimens were then sliced in coronal sections using a brain matrix and sent to the pathology laboratory for hematoxylin and eosin staining.

Image processing

Histological slides depicting the largest tumour area on pathology were selected for each animal, digitized and compared with the corresponding MR image. Both images were analyzed using the image processing software "SigmaScan Pro 5" (Hallogram Publishing, Aurora, USA). The tumour contour was manually drawn for the pathology slides, whereas the enhancement signal on T1 was drawn for the MR images. The software calculated area measurements in mm^2 after conversion and standardization from pixel units (Figure 2).

Results

Tumour was observed in each animal and produced a bright and homogeneous enhancement. Enhanced T1 images were used to calculate tumour surface, as there was a clear demarcation between enhancing tumour and surrounding brain. Analysis of enhancing signal on MRI produced the following surface measurements: 2.18 mm^2 ± 0.91 at five days, 8.25 mm^2 ± 0.91 at ten days, 21.6 mm^2 ± 2.38 at 15 days and 23.17 mm^2 ± 2.56 at 20 days. The T2 images allowed a clear recognition of anatomical structures, such as the ventricules and basal ganglia. It also depicted the mass effect and shift in the midline caused by the tumour. The interface between tumour and normal brain was blurred, without a clear margin on the T2 sequences.

Tumour margin evaluation on pathologic samples generated surfaces of 0.29 mm^2 ± 0.2 at five days, 4.43 mm^2 ± 0.89 at ten days, 8.3 mm^2 ± 0.22 at 15 days and 12.9 mm^2 ± 0.45 at 20 days. For all the animals assessed, a good match between radiology and pathology regarding the topographic distribution of the tumours was found (Figure 3). However, although a parallel increase in tumour areas was noted on both the histological sample and the MR scan for every animal, a significant discrepancy was obvious, with the MR surfaces significantly greater than the histological surfaces. This overestimation was present in every subject in a constant fashion. As can be appreciated from the data, the histology samples depicted a

https://doi.org/10.1017/S0317167100004753 Published online by Cambridge University Press

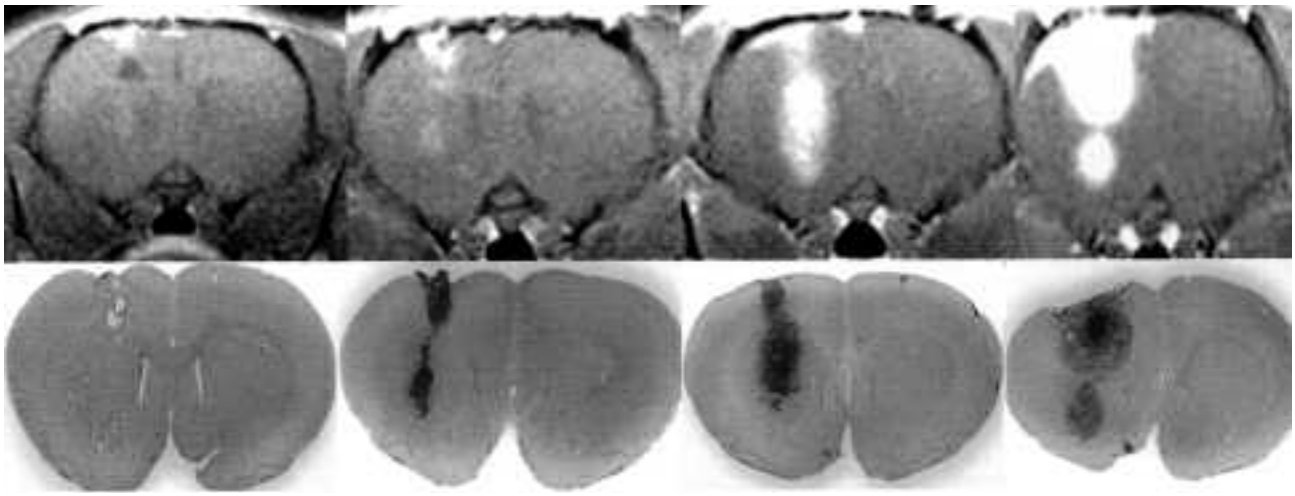

Figure 3: *Tumour size progression, as exemplified by MR obtained in four animals from each time group (five, ten, 15 and 20 days post implantation). Similitude in morphology and size between radiology and pathology is obvious.*

consistency in the calculated areas, whereas the MR data was more variable.

Discussion

A multiplicity of rat glioma models have been described in the literature. Each of these models displays different characteristics rendering them unique. We elected to work with the F98/Fischer model because it regroups some of the characteristics which we think are essentials in the establishment of a valid glioma model.[20] The F98 cell line was developed at Ohio State University by a single dose of ENU administered to a pregnant Fischer rat.[21] This model is characterized by an infiltrative growth pattern and histopathological morphology matching that of an anaplastic glioma.[22] It is also very weakly immunogenic when used with its syngeneic host, the Fischer rat.[23]

In improving the validity of data acquired through these experimental models, in vivo assessment modalities are essential to monitor responses of experimental treatment strategies and to allow radiological follow-up of the animals.[12] The F98 model has already been studied with MRI, but only using experimental high field magnets.[24,25] Other glioma models have been studied using regular magnet with commercially available antenna.[11] However, these studies are scarce, and most recently published works focus on the use of either high-field experimental magnets, and/or custom made antennas.[13-16] While there is no denying that these technologies are worthwhile and useful, they are expensive and are not readily available to most laboratories.[11] Moreover, even though these high field magnet units can be used to gain greater insight in the physiology and the biological behaviour of a tumour and its surrounding (Blood brain barrier (BBB) integrity, brain around tumour vascularisation and so on), they might not be necessary to study tumour progression and response to various treatment strategies.[11] To do so, we believe that a human MR with a commercial antenna can lend images of adequate resolution.

In this study, adequate T1 sequences were obtained for the entire population of animals imaged, enabling successful tumour surface quantification using T1 enhanced sequences. We used a small coil antenna that was simply laid on the head of the animal, thus maximizing signal strength. Although we also tested images in axial and sagittal sequences, only the coronal plane was later routinely imaged, given that no additional data was gained with the other planes. The surface measurements obtained showed a gradual increase with time to implantation, as was expected (Figure 3). However we found an overlap of standard deviations

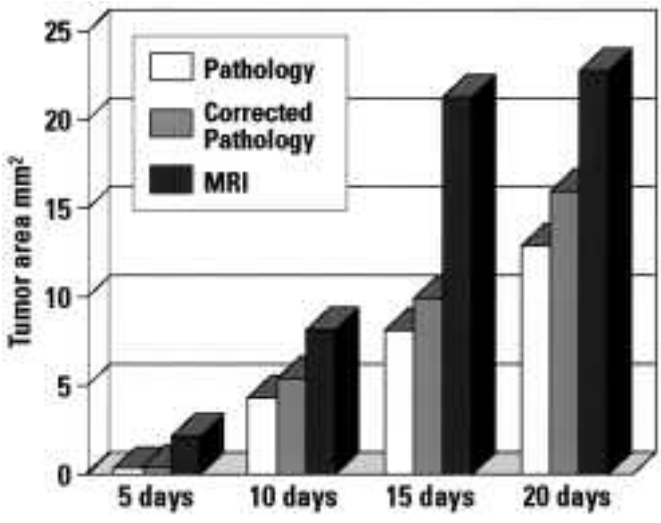

Figure 4: *Graphic plotting mean tumour areas as calculated for the pathology samples and the MR scans. The pathological areas are also expressed after correction of the shrinkage factor as calculated in this study.*

https://doi.org/10.1017/S0317167100004753 Published online by Cambridge University Press

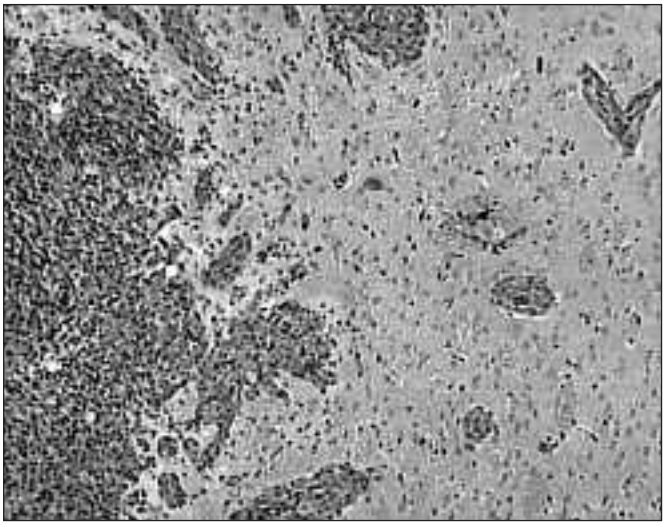

Figure 5: 40X pathological magnification at the periphery of the tumour nodule, depicting neo vascularisation in the area of the brain around tumour (BAT).

in this set of data. The small sample size, and the short interval time between each group imaged likely contribute to this phenomenon. Comparing tumour surfaces using longer interval times would have led to statistically significant results.

The present study was also designed to assess the relationship in tumour morphology and topography between the pathology sample and T1-enhancing images obtained in corresponding animal. Ultimately, we intended to ensure the validity of this imaging technique in following in vivo tumour growth.

As expected, tumour areas as measured by MR imaging showed a gradual increase in time, which parallels the pathological findings. However, when looking at the data, we found a constant overestimation of tumour size with MR imaging. Many factors could explain this discrepancy. It is a well known fact that tissue fixation and processing with formalin and paraffin cause shrinkage due to dehydration. The shrinkage factor reported is highly variable, ranging from 7% to 33% in the literature.[26,27] This variation is probably explained by differences in the fixation techniques. Different methods have been described to measure the shrinkage factor.[28] To establish this factor in the present study, we elected to measure the entire brain surfaces on MR imagery and on the corresponding pathological slides in three randomly selected rats. The images were analyzed using the image processing software as described in the methods section. Corresponding images were manually contoured for brain area calculation, expressed as pixel units. These surface calculations were averaged, and a ratio pathology sample/ MRI of 0.84 was calculated. The shrinking factor was thus estimated at 16%. When this correction factor was applied to the results, the correspondence between the two modalities was improved (Figure 4). Even though the shrinking factor explains some of the difference evidenced between the pathology sample and the MR image, other mechanisms are active in producing this discrepancy.

One such factor is the phenomenon of neovascularisation at the brain around tumour area. The F98 tumours produced by our implantation technique are characterized by an endothelial proliferation that extends beyond the tumour nodule into a zone of adjacent brain infiltration, the so-called brain around tumour area (Figure 5). This phenomenon is tributary to the invasive behavior of the F98 cells, and emulates the human situation of a malignant astrocytoma.[29] These new capillaries lack tight junctions, which render them permeable to macromolecules. This altered permeability is the basis of enhanced imaging, but can lead to overestimation of tumour size, because the enhancing signal might include the brain around tumour area.

Tumour proliferation in the subdural compartment is yet another mechanism contributing to the discrepancy between the pathology samples and corresponding imaging by MR. In certain imaging samples, it appears that tumour cells proliferated into the subdural space (Figure 6). This phenomenon has been described in countless reports, and is related to the implantation process. More specifically, the leptomeningeal puncture and the needle tract produced by the implantation technique are physical anomalies through which the tumour cells can backtrack and produce subdural tumour growth. Despite our efforts to eradicate this problem by using a small infusion volume, slowly retracting the needle and sealing the craniotomy with bone wax, we still occasionally encounter significant extra-axial tumour growth. When analyzing the MR images, it is impossible to accurately separate this growth from the main tumour nodule. However, when harvesting the brain, this extra-axial growth is inevitably removed with the dura. Thus, the MR surface calculation results include this artifact which is absent from the pathological surface calculations (Figure 6).

As animal models are increasingly used to assess in vivo efficacy of different therapies, a need to devise in vivo imaging strategies in these models has emerged. Numerous models are in use, and significant variation in the tumour take, growth pattern and survival time of the animals are reported. This study reports our findings in assessing radiologically F98-implanted Fischer rats with a commercial magnet and antenna, using a standardized implantation technique. Although the MR scans consistently overestimated the actual tumour size, the radiological tumour growth reported in this study paralleled the histological samples. This technology is thus suitable to follow in vivo tumour growth of animals exposed to a standardized implantation technique in which a treatment modality needs to be assessed, keeping in mind the limitations imposed by this overestimation.

Acknowledgments

The authors thank Ms. Cecile Langford for her help and enthusiasm during this project. This project was supported by a grant from the Cancer Research Society, and a resident research grant from the surgery department of the Sherbrooke University.

References

1. Binder DK, Keles GE, Aldape K, Berger MS. Aggressive glial neoplasms. In: Batjer HH, Loftus CM, editors. Textbook of neurological surgery, principles and practice, Philadelphia: Lippincott Williams & Wilkins; 2003. p. 1270-80.
2. Walker MD, Alexender E Jr, Hunt WE, et al. Evaluation of BCNU and/or radiotherapy in the treatment of anaplastic gliomas. J Neurosurg. 1978;49:333-43.

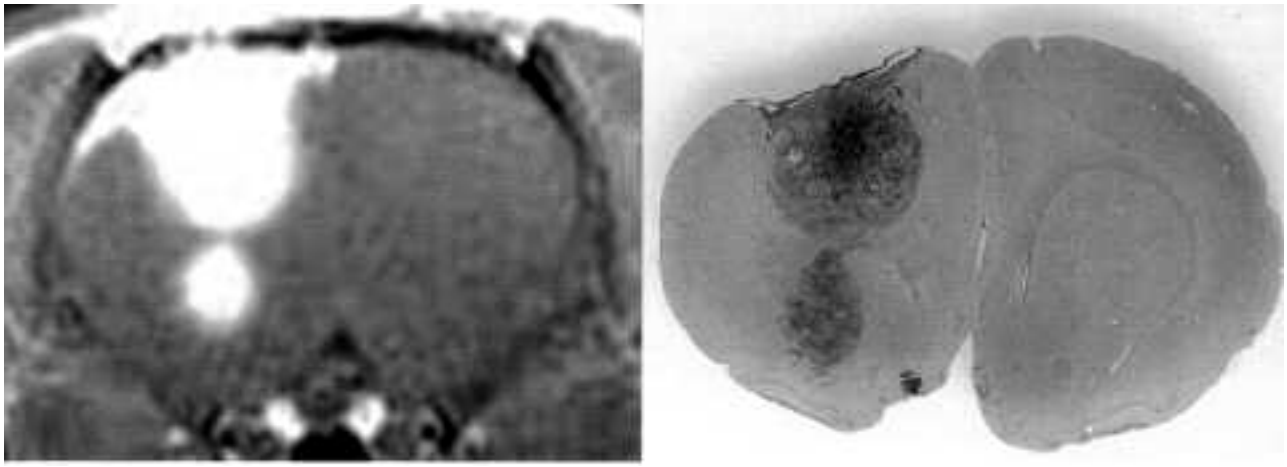

Figure 6: *The MR image and pathological slide of an animal subject at 20 days after implantation. The MRI shows a subdural mass in continuity with the main tumour nodule. On pathological slide, this subdural mass was inevitably removed with the dura during the harvesting of the brain. A depression is observed on the brain surface corresponding to the imprint of the subdural mass.*

3. Dilmanian FA, Button TM, Le Duc G, et al. Response of rat intracranial 9L gliosarcoma to microbeam radiation therapy. Neuro-Oncology. 2002;4(1):26-38.
4. Fournier E. Passirani C. Montero-Menei C, et al. Therapeutic effectiveness of novel 5-fluorouracil-loaded poly(methylidene malonate 2.1.2)-based microspheres on F98 glioma-bearing rats. Cancer. 2003;97(11):2822-9.
5. Pavillard V, Kherfellah D, Richard S, et al. Effects of the combination of camptothecin and doxorubicin or etoposide on rat glioma cells and camptothecin-resistant variants. Br J Cancer. 2001;85(7):1077-83.
6. Jean WC, Spellman SR, Wallenfriedman MA, et al. Interleukin-12-based immunotherapy against rat 9L glioma. [Journal Article] Neurosurgery. 1998;42(4):850-6.
7. Gridley DS, Baer JR, Cao JD, et al. TNF-alpha gene and proton radiotherapy in an orthotopic brain tumor model. Int J Oncol. 2002;21(2):251-9.
8. Weyerbrock A, Walbridge S, Pluta RM, et al. Selective opening of the blood-tumor barrier by a nitric oxide donor and long-term survival in rats with C6 gliomas. J Neurosurg. 2003;99:728-37.
9. Wilkins DE, Raaphorst GP, Saunders JK, et al. Correlation between Gd-enhanced MR imaging and histopathology in treated and untreated 9L rat brain tumors. Magn Reson Imaging. 1995;13;1:89-96.
10. San-Galli F, Vrignaud P, Robert J, et al. Assessment of the experimental model of transplanted C6 glioblastoma in Wistar rats. J Neurooncol. 1989;7(3):299-304.
11. Raila FA, Bowles AP, Perkins E, Terrell A. Sequential imaging and volumetric analysis of an intracerebral C6 glioma by means of a clinical MRI system. J Neurooncol. 1999;43:11-17.
12. Thorsen F, Ersland L, Nordli H et al. Imaging of experimental rat glioma using a clinical MR scanner. J Neuroncol. 2003;63:225-31.
13. Kish EP, Blaivas M, Strawderman M et al. Magnetic resonance imaging of ethyl-nitrosourea-induced rat glimas: a model for experimental therapeutics of low-grade gliomas. J Neurooncol. 2001;53:243-57.
14. Ross BD, Zhao YJ, Neal ER, et al. Contributions of cell kill and posttreatment tumor growth rates to the repopulation of intracerebral 9L tumors after chemotherapy: an MRI study. Proc Natl Acad Sci USA. 1998;95:7012-17.
15. Le Duc G, Péoc'h M, Rémy C, et al. Use of T2-weighted susceptibility contrast MRI for mapping the blood volume in the glioma-bearing rat brain. Magn Reson Med. 1999;24:754-61.
16. Nelson AL, Algon SA, Munasinghe J, et al. Magnetic resonance imaging of patched heterozygous and xenografted mouse brain tumors. J Neurooncol. 2003;62:259-67.
17. Schmiedl UP, Kenney J, Maravilla KR, Kinetics of pathologic blood-brain-barrier permeability in an astrocytic glioma using contrast-enhanced MR. Am J Neuroradiol. 1992;13:5-14.
18. Kenney J, Schmiedl U, Maravilla K, et al. Measurement of blood-brain barrier permeability in a tumor model using magnetic resonance imaging with gadolinium-DTPA. Magn Reson Med. 1992;27:68-75.
19. Yunting Z, Jianling C, Xuwen L, et al. MR imaging in rat glioma model and gene therapy using EGFR antisense RNA. Chin Med J (Engl). 1998;11:993-7.
20. Mathieu D, Lamarche JB, Fortin D. The importance of a syngeneic glioma implantation model: The F98/Fischer rat model. Can J Neurol Sci. 2002; A-05 Suppl S1–9.
21. Ko L, Koestner A, Wechsler W. Morphological characterization of nitrosourea-induced glioma cell lines and clones. Acta Neuropathol. 1980;51:23-31.
22. Kobayashi N, Allen N, Clendenon NR, Ko L. An improved rat brain-tumor model. J Neurosurg. 1980;53:808-15.
23. Tzeng JJ, Barth RF, Orosz CG, James SM. Phenotype and functional activity of tumor-infiltrating lymphocytes isolated from immunogenic and nonimmunogenic rat brain tumors. Cancer Res. 1991;51:2373-8.
24. Eis M, Els T, Hoehn-Berlage M. High resolution quantitative relaxation and diffusion MRI of three different experimental brain tumors in rat. Magn Reson Med. 1995;34:835-44.
25. Ernestus RI, Wilmes LJ, Hoehn-Berlage M. Identification of intracranial liqor metastases of experimental stereotactically implanted brain tumors by tumor-selective MRI contrast agent MnTPPS. Clin Exp Metastasis. 1992;10:345-50.
26. Wree A, Goller HJ, Beck T. Local cerebral glucose utilization in perfusion-fixed rat brains. J Neurosci Methods. 1995;58:143-9.
27. Bancroft JD, Stevens A, editors. Theory and practice of histological techniques. 4th edition. Edinburgh; Churchill Livingstone; 1996.
28. Prabhu SS, Broaddus, WC, Oveissi C, et al. Determination of intracranial tumor volumes in a rodent brain using magnetic resonance imaging, evans blue, and histology: a comparative study. IEEE Trans Biomed Eng. 2000;47:2; 259-65.
29. Barth RF. Rat brain tumor models in experimental neuro-oncology: the 9L, C6, T9, F98, RG2 (D74), RT2 and CNS-1 gliomas. J Neurooncol. 1998;36:91-102.